DOI: 10.1002/cbdv.202000272

FULL PAPER

CHEMISTRY & BIODIVERSITY

Redirection of miRNA-Argonaute Complexes to Specific Target Sites by Synthetic Adaptor Molecules

Mathias Bolz,[a] Laura Thomas,[b] Ute Scheffer,[a] Elisabeth Kalden,[a] Roland K. Hartmann,[b] and Michael W. Göbel*[a]

[a] Institute of Organic Chemistry and Chemical Biology, Goethe University Frankfurt, Max-von-Laue-Str. 7, DE-60438 Frankfurt, Germany, e-mail: m.goebel@chemie.uni-frankfurt.de

[b] Institute of Pharmaceutical Chemistry, Philipps University Marburg, Marbacher Weg 6–10, DE-35032 Marburg, Germany

Dysregulation of miRNAs is connected with a multitude of diseases for which antagomirs and miRNA replacement are discussed as therapeutic options. Here, we suggest an alternative concept based on the redirection of RISCs to non-native target sites. Metabolically stable DNA-LNA mixmers are used to mediate the binding of RISCs to mRNAs without any direct base complementarity to the presented guide RNA strand. Physical redirection of a dye-labeled miRNA model and of specific miRNA-programmed RISC fractions present in HeLa extracts is demonstrated by pull-down experiments with biotinylated capture oligonucleotides.

Keywords: argonaute proteins, locked nucleic acids, RNA induced silencing complex, pull-down, Western blot, mRNA, RNA recognition.

Introduction

MicroRNAs[1–10] (miRNAs) and small interfering RNAs[11–14] (siRNAs) are short non-coding RNAs with a strand length of *ca.* 22 nucleotides. Embedded into Argonaute proteins they form RNA-induced silencing complexes (RISC), important negative regulators of translation. The phenomenon of RNA interference is based on RISCs binding to a fully complementary mRNA. The Argonaute 2 subtype will then cleave the target strand in a catalytic fashion by its RNase H endonuclease activity.[15,16] RISCs of miRNAs only partially base-pair with their targets and usually do not directly cleave mRNAs. For some exceptions, see ref. [17]. Binding to the 3′ untranslated region (3′-UTR) of mRNAs results in translational arrest and also induces degradation of the RNA target (*Scheme 1,a*).[1–10] This mechanism seems to affect a large fraction of all human genes.[18–21]

Dysregulation of miRNA pathways is associated with disease, in particular with cancer.[22–24] For example, increased levels of the miRNA cluster 17–92 are found in many types of malignancies.[25] Processing of the primary transcript leads to six mature miRNAs: miR-17, miR-18a, miR-19a, miR-19b–1, miR-20a and miR-92. A common mechanism of these 'oncomirs' is downregulation of tumor suppressors, for example RB1 or TGFBR2.[23] Such pathogenic effects can be corrected by antagomirs,[26] or by short LNAs (locked nucleic acids) and other oligonucleotides complementary to the seed region of the miRNA (*Scheme 1,b*).[27–34] A lack of specific miRNAs can also contribute to disease. For such cases, delivery of miRNA mimics has been explored as a therapeutic substitution approach.[24,32–38] However, synthetic miRNA mimics like siRNAs are susceptible to enzymatic degradation. Enhancing the stability by structural modifications[39–48] is not trivial because many modifications impair mRNA silencing ability. Therefore, improving the formulation with delivery agents has been the preferred way to increase the efficacy of miRNA mimics. First clinical trials – in part successful –

Supporting information for this article is available on the WWW under https://doi.org/10.1002/cbdv.202000272

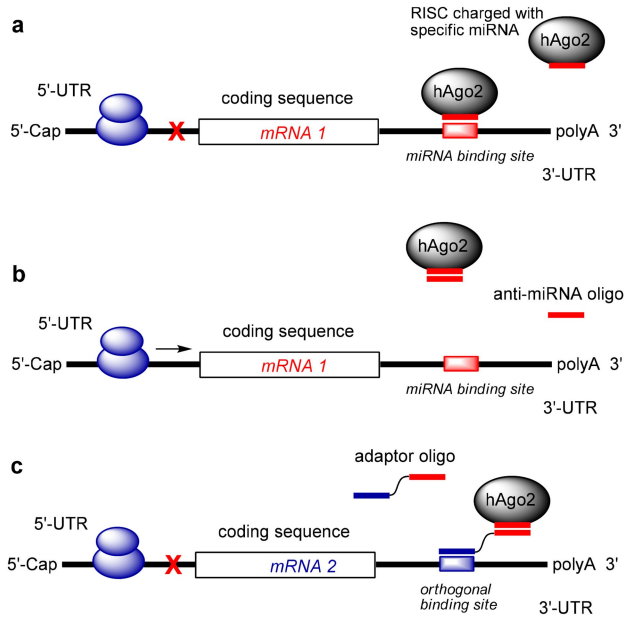

Scheme 1. General concept of RISC redirection by adaptor oligonucleotides. a) A RISC binds to the 3′-UTR of mRNA 1: translation is repressed. The miRNA and the miRNA binding site are shown in red. b) An anti-miRNA oligo hybridizes with the RISC and prevents binding to the 3′-UTR: translation of mRNA 1 is increased. c) The 'red' part of a bifunctional LNA adaptor displaces the RISC from mRNA 1 while the 'blue' part redirects it to the 3′-UTR of a specific mRNA 2: translation of mRNA 2 should be repressed (ribosomes are represented by blue ovals).

have also seen severe immune-related off-target effects.[33,38] Most recently, conjugates of a cationic peptide and a PNA (peptide nucleic acid) complementary to the oncogenic miR-21 could be used to co-deliver a miR-34a mimic into HeLa cells thus combining the two concepts of miRNA antagonists and miRNA substitution.[49]

RISCs are known to associate with glycine-tryptophan-rich GW proteins such as TNRC6 which further recruit the machinery responsible for translational arrest, deadenylation and mRNA decay.[50] It is important to note that these mechanisms do not require a precise localization of RISC binding – in contrast to mRNA cleavage by siRNAs. All effects of miRNAs on 3′-UTRs are assumed to be mediated by protein–protein interactions through space. This property offers the chance not only to block the adverse effects of overexpressed miRNAs by complementary oligonucleotides (antimiRs),[26–34] but to redirect specific RISCs with an adaptor molecule to a second pathogenic mRNA to inhibit its expression. The adaptor associates at one end with a RISC-bound miRNA and at the other end with the specific target mRNA by *Watson-Crick* base pairing (*Scheme 1,c*). Therefore, this approach is free from the structural restrictions (limited modifiability) pertaining to siRNAs and miRNA mimics. Here we show by pull-down experiments that bifunctional LNAs can act as non-degradable adaptor molecules that have the ability to redirect RISC complexes to a new specific RNA target.

Hybridization of the adaptor oligonucleotide with RISCs by the complementary 'red' part will first of all interfere with RISC binding to the normal target. Like the anti-miRNA oligo shown in *Scheme 1,b*, it may cause reactivation of repressed mRNAs. The pending 'blue' part of the adaptor may then hybridize with a complementary second mRNA and thus redirect the RISC to a new target (*Scheme 1,c*).

Results and Discussion

To illustrate the concept, we performed some band shift studies and initial pull-down experiments with oligonucleotides **1**–**3** (*Figure 1,a*). Compound **1** is a dye-labeled, protein-free model of miR-20a. It is not complementary to the biotinylated capture oligo **3**, but it can be indirectly tethered to oligo **3** by base-pairing with adaptor oligonucleotide **2** (*Figure 1,b*). The latter consists of two 14-meric LNA/DNA mixmer moieties connected by a hexaethyleneglycol (HEG) linker. The long and hydrophilic linker was chosen to reduce steric hindrance and to avoid hydrophobic

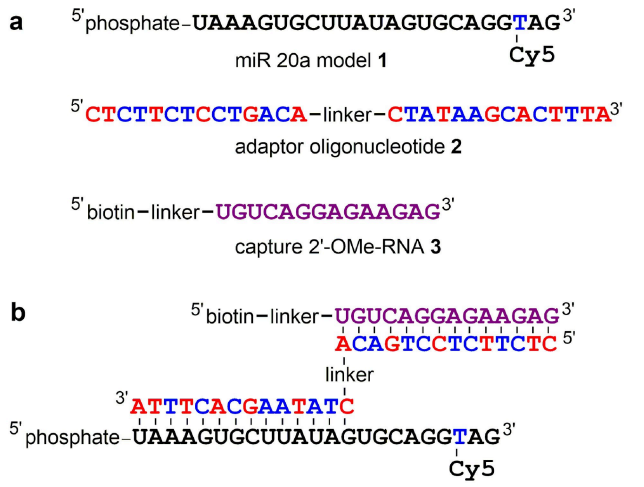

Figure 1. Oligonucleotides used for pull-down experiments (black: RNA; blue: DNA; red: LNA; magenta: 2′-OMe RNA; linker: hexaethyleneglycol). a) miR-20a model **1** binds to adaptor oligo **2**, but not to capture oligo **3**. b) Adaptor oligo **2** should mediate binding of the miR model to the biotinylated capture oligo **3** or to analogous RNA sequences in a ternary complex.

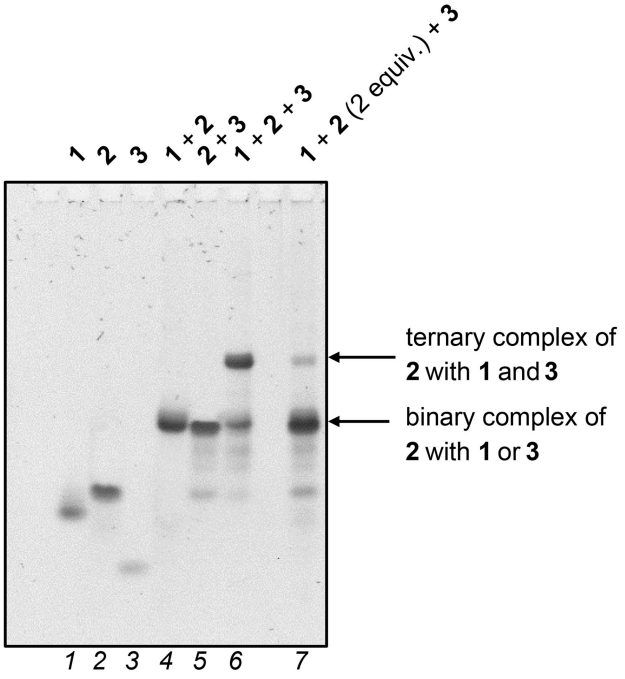

Figure 2. Band shift experiments with oligonucleotides **1**–**3**. *Lane 1*: miRNA model **1**; *lane 2*: adaptor oligo **2**; *lane 3*: capture oligo **3**; *lane 4*: RNA **1** + adaptor **2** (1 : 1); *lane 5*: adaptor **2** + oligo **3** (1 : 1); *lane 6*: RNA **1** + adaptor **2** + oligo **3** (1 : 1 : 1); *lane 7*: RNA **1** + adaptor **2** + oligo **3** (1 : 2 : 1). The gels were stained with *SYBR Gold*.

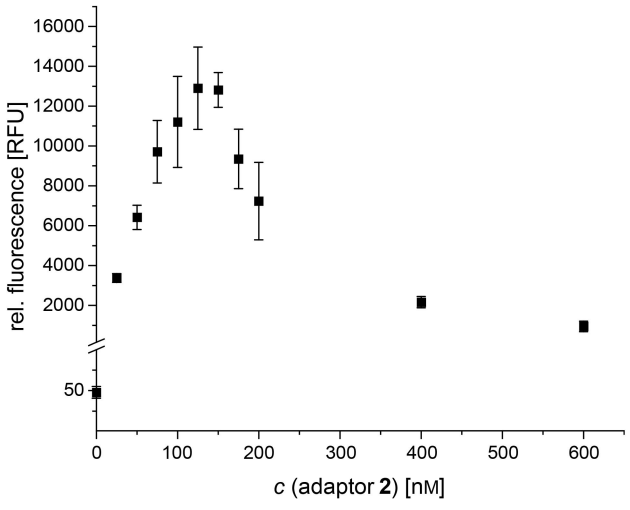

Figure 3. Pull-down of dye-labeled miRNA model **1** (100 nM) by capture oligo **3** (100 nM) in the absence and presence of adaptor oligo **2**. At a 1 : 1.25 : 1 ratio of all three oligonucleotides, a 270-fold gain in fluorescence was observed. At higher concentrations of **2**, formation of binary complexes was favored and the capture of **1** became less effective. The data points represent the mean values of three independent experiments (± SD).

contraction. When adaptor **2** was mixed with either oligo **1** or **3**, hybridization was indicated by a clear shift of electrophoretic bands (*Figure 2*, *lanes 4* and *5*). In the presence of all three oligos in equimolar amounts, a slower migrating band representing the ternary complex became the major species. Doubling the concentration of adaptor **2** weakened this band: Excessive amounts of **2** will stay uncomplexed or form 1 : 1 hybrids, either with oligo **1** or **3**.

For pull-down experiments, the biotinylated capture oligo **3** (100 nM) was bound to streptavidin-coated magnetic beads, miRNA model **1** (100 nM) was added, followed by addition of adaptor **2** in concentrations from 0 to 600 nM. After pull-down, the beads were thoroughly washed, and duplexes were dissociated by addition of NaOH. The amount of captured RNA **1** was finally quantified by fluorescence (*Figure 3*). In the absence of adaptor **2**, no binding of RNA **1** to the noncomplementary capture oligo **3** was expected. Accordingly, a low level of fluorescence was observed. Upon stepwise addition of **2**, fluorescence increased, went through a maximum and then decreased again. The capture of RNA **1** was most effective at a ratio of oligos close to 1 : 1 : 1, where a 270-fold increase in fluorescence was observed compared to the low initial value in the absence of adaptor **2**. At higher concentrations of **2**, the probability of forming ternary complexes is increasingly disfavored as already seen in the band shift assay (*Figure 2*).

A second adaptor **4** was synthesized to redirect miR-20a to an accessible binding site within the 3′-UTR of the *PIM1* mRNA (*Figure 4,a*).[51,52] This oligonucleotide was tested by band shift and pull-down experiments with miRNA model **1** and a new capture oligo **5**, mimicking the *PIM1* mRNA. The results, however, differed from those shown above in *Figures 2* and *3*. Apart from the weak stainability of capture oligo **5** (*Figure 4,c*, *lane 3*), a substantial fraction of the three oligos still assembled into the ternary complex at a twofold excess of adaptor **4**, which differs from the behavior of oligos **1**–**3**. We explain this effect by partial self-complementarity of adaptor **4** (*Figure 4,b*), which is in line with adaptor **4** migrating faster in the native gel than RNA **1**, although the latter is shorter than adaptor **4** (*Figure 4,c*, *lanes 1* and *2*). Binding to either RNA **1** or oligo **5** seems to open up the hairpin structure, thereby facilitating binding of the second oligonucleotide. When the pull-down experiment shown in *Figure 3* was repeated with adaptor **4**, the highest amounts of recovered RNA **1** were found at a 1 : 1.5 : 1 ratio of oligonucleotides (*Figure 5*). Consistent with facilitated binding of miRNA model **1** to the

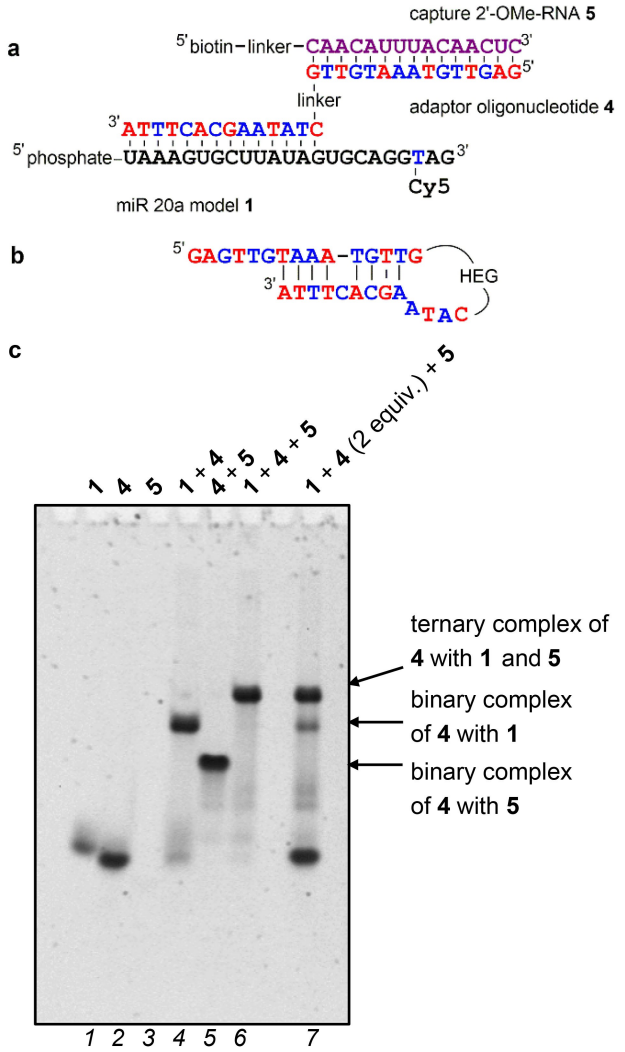

Figure 4. a) Ternary complex of oligonucleotides **1**,**4**, and **5**. b) Possible self-structure of adaptor oligo **4**. c) Band shift experiments. *Lane 1*: miRNA model **1**; *lane 2*: adaptor **4**; *lane 3*: capture oligo **5**; *lane 4*: RNA **1** + adaptor **4** (1 : 1); *lane 5*: adaptor **4** + capture oligo **5** (1 : 1); *lane 6*: RNA **1** + adaptor **4** + oligo **5** (1 : 1 : 1); *lane 7*: RNA **1** + adaptor **4** + oligo **5** (1 : 2 : 1). The gels were stained with *SYBR Gold*.

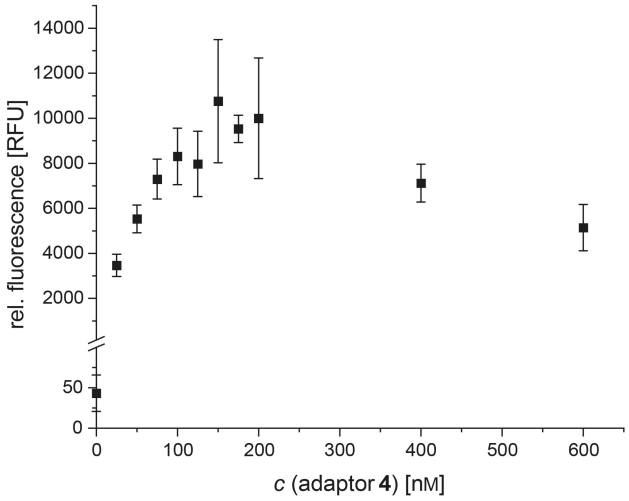

Figure 5. Pull-down of dye-labeled miRNA model **1** (100 nM) by capture oligo **5** (100 nM) in the absence and presence of adaptor oligo **4**. At a 1 : 1.5 : 1 ratio of all three oligonucleotides, a 250-fold gain in fluorescence was observed. At increasing concentrations of **4**, the loss of fluorescence (corresponding to the concentration of the ternary complex) was less pronounced than in *Figure 3*. The data points represent the mean values of three independent experiments (± SD).

binary complex of oligo **5** and adaptor **4**, the pull-down yield of dye-labeled RNA **1** upon increasing concentrations of adaptor **4** dropped less steeply than in *Figure 3*. We also conducted some melting experiments to test if the self-complementarity of adaptor **4** might weaken the interaction with the target strands. However, the duplex stabilities when miRNA model **1** is bound to adaptor **2** or **4**, or to oligo **6** which represents only the 3′ half of adaptors **2** and **4**, were quite similar (*Figure 6*). Correspondingly, identical melting points were observed for duplexes of capture oligo **5** and adaptor **4** or oligo **7**, representing the 5′ half of adaptor **4**. Increased thermal stability due to its higher G–C content was detected for the duplex **2:3**. A clear hint for self-complementarity was seen in the melting profile of adaptor **4** itself showing sigmoidal behavior with points of inflection around 32 and 62 °C. (*Supporting Information*).

Having established the function of adaptors **2** and **4**, we turned next to cell extracts. The isolation and purification of active RISCs from cells was previously achieved by incorporating 3′ biotinylated guide strands into Argonaute proteins, pull-down with streptavidin beads and photochemical removal of the biotin part.[39] Specific RISCs can also be captured by hybridization of guide RNA-programmed RISCs with biotinylated oligonucleotides.[53,54] High duplex stabilities are observed with fully complementary partner strands. Thus, recovery of RISCs under native conditions may become difficult[28] unless special protocols are followed.[53] Nonetheless, for implementation of the redirection strategy outlined in *Scheme 1*, these findings are encouraging.

For isolation of RISCs, we used lysates of HeLa cells known to express both micro RNAs 20a and let-7a. In the first part of the experiments the cytosolic fraction of cell lysates was incubated with an excess of capture LNA **8** bound to magnetic beads. After pull-down, the protein part was removed from the beads and

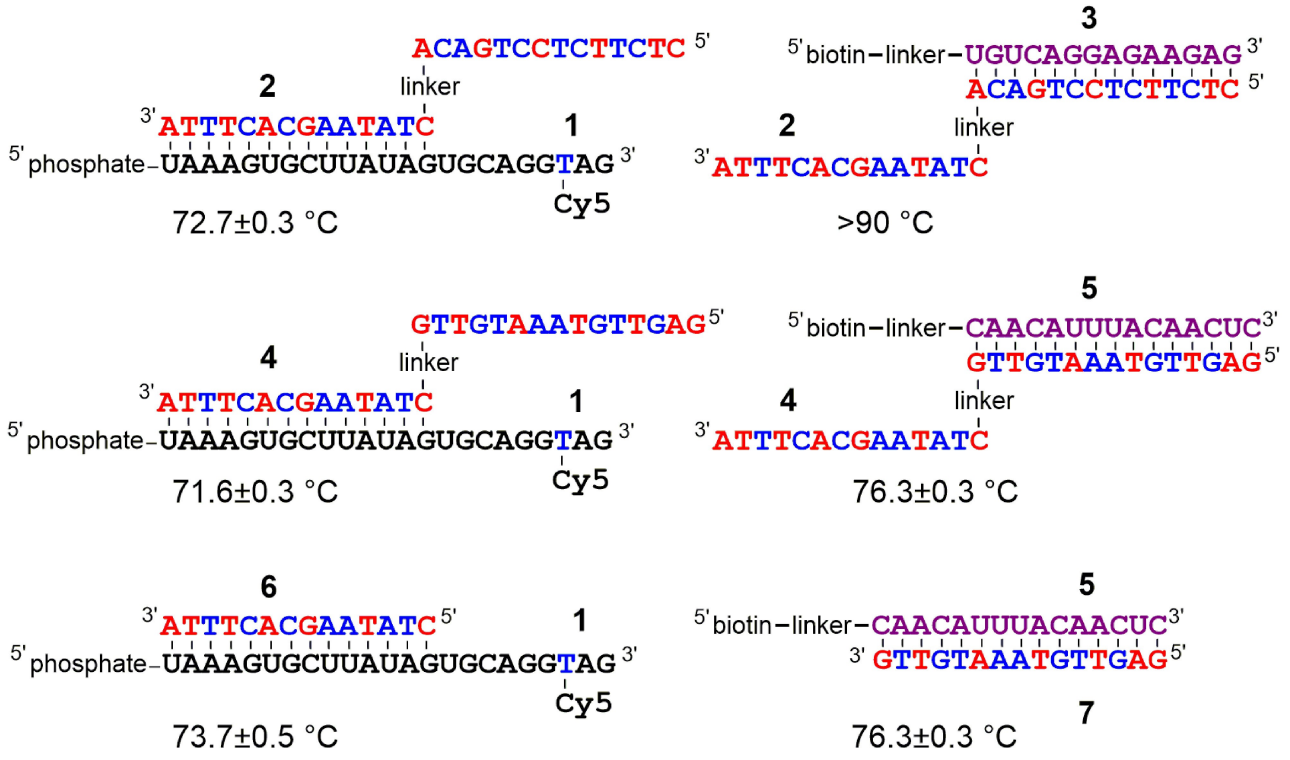

Figure 6. Thermal denaturation of duplexes formed by adaptors **2** and **4** and comparison with oligonucleotides **6** and **7**, representing the two fragments of adaptor **4** (data is shown in the *Supporting Information*). The oligonucleotides (1 μM) were incubated in 1 mL of buffer (100 mM KCl, 2 mM $MgCl_2$, 50 mM *Tris*·HCl pH 8) for 20 h at 37 °C. The absorption at 260 nm was measured in a range from 20 °C to 90 °C. The melting points are the mean values (±SD) from three to five independent denaturation/renaturation cycles.

separated by gel electrophoresis. Western blotting with antibodies against hAgo2 showed a strong band around 100 kDa corresponding well to the known size of this protein (*Figure 7*, *lane 1*). *Lane 2* shows a repetition of the pull-down step using the same sample of cell lysate. A much weaker band was visible indicating depletion of miR-20a-loaded RISCs. The cell lysate was extracted again but this time with an excess of capture LNA **9**, complementary to let-7a. *Lane 3* shows a strong hAgo2 signal. A second pull-down with LNA **9** again isolated much less material (*lane 4*): The capture process looks exhaustive for defined fractions of RISCs, thus providing evidence for specific base pairing between miRNAs and LNAs.

In the redirection experiment (*Figure 8*), we replaced LNA **8** by capture 2′-OMe-RNA **3** (see *Figure 1*). This oligonucleotide represents the target mRNA 2 shown in *Scheme 1,c* and is stabilized against fast enzymatic degradation in the cell lysate. The capture oligo **3**, although not complementary to miR-20a, might accidentally bind some other microRNAs. Thus, we were pleased to find not more than a very faint

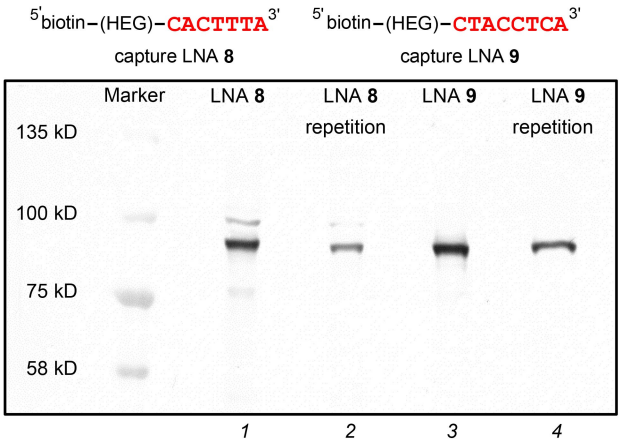

Figure 7. Isolation of RISCs by pull-down with LNAs **8** and **9**, complementary to the seed regions of miR-20a and let-7a; visualization by Western blot after electrophoretic separation of proteins, using an antiserum specific for human Ago2 (hAgo2). *Lane 1*: HeLa cell lysate and LNA **8**. *Lane 2*: Repetition of this step with LNA **8**. *Lane 3*: Repetition of this step with LNA **9**. *Lane 4*: Second repetition of this step with LNA **9**.

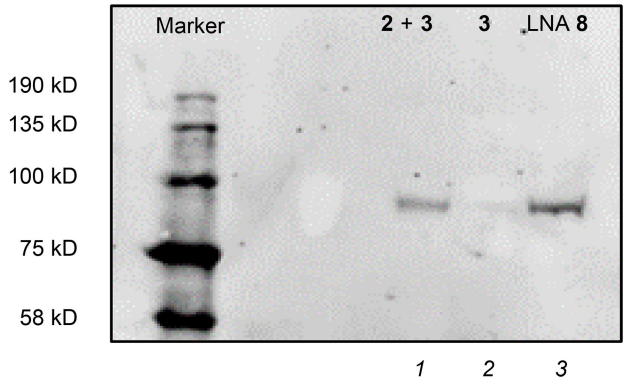

Figure 8. Isolation of RISCs by pull-down with capture 2′-OMe-RNA **3** in the absence or presence of adaptor oligo **2**. Visualization by Western blot after electrophoretic separation of proteins using an antiserum specific for hAgo2. *Lane 1*: HeLa cell lysate with capture RNA **3** and adaptor **2**. *Lane 2*: HeLa cell lysate with capture RNA **3**. *Lane 3*: HeLa cell lysate with capture LNA **8** used as positive control.

band of hAgo2 in the Western blot (*Figure 8*, *lane 2*). However, in the presence of adaptor **2**, pull-down with capture oligo **3** resulted in a much stronger hAgo2 Western blot signal (*Figure 8*, *cf. lanes 1* and *2*). For direct capturing, LNA **8** was used as a positive control (*Figure 8*, *lane 3*). Our results demonstrate tethering of miR-20a charged RISCs to a new target RNA through a bifunctional adaptor molecule.

We have attempted to apply our approach to the redirection of RISCs within HeLa cells after transfection of adaptor oligonucleotides. Yet, the results obtained so far have not been conclusive. Among the many possible reasons, one could be a low frequency of ternary complex formation between miRNA-programmed RISC, adaptor oligo and the new target mRNA in the crowded and compartmentalized intracellular environment.

Conclusions

In theory, the concept of RISC redirection shown in *Scheme 1,c* has several attractive features. It resembles the miRNA replacement approach but avoids the disadvantage of restricted modifiability of miRNA mimics, because the adaptor is not incorporated into Argonaute protein complexes but solely needs to hybridize with the miRNA strand presented by the RISC. Thus, different types of oligonucleotides are eligible as adaptors. At the same time, adverse effects of overexpressed miRNAs such as oncomirs may be antagonized (*Scheme 1,b* and *1,c*). Furthermore, the effect of RISC redirection should be more pronounced in cell types overexpressing the target miRNA. It is of course a question of stoichiometry if an adaptor can down-regulate one gene and up-regulate others simultaneously. When fluorescently labeled miRNA model **1** was redirected using adaptor **2**, a ratio close to 1 : 1 : 1 was found optimal (*Figure 3*). Both, a lack but also an excess of adaptor effectively reduces the fraction of ternary complexes. At first glance, when compared to adaptor **2**, oligonucleotide **4** may appear suboptimal because self-complementarity of the adaptor will slightly weaken the formation of complexes with miRNAs and mRNAs at equimolar concentrations of all three components. However, *Figure 5* also illustrates a positive effect resulting from binding cooperativity: Even when the system is over-titrated with an excess of adaptor **4**, high amounts of ternary complexes are still present. We do not know at the moment if low levels of adaptor self-complementarity might be detrimental in cell culture experiments or even helpful, but it is an interesting aspect that should be kept in mind. Here, we can only present a first step towards a practical use of RISC redirection. *Figure 7*, however, provides evidence that capture of miRNA-programmed RISCs from cell lysates with LNAs occurs in a sequence-specific manner. *Figure 8* finally shows that miRNA redirection works, at least *in vitro*, not only with isolated RNA strands but also with complete RISCs.

Experimental Section

General

LNA oligonucleotides, mixmers and 2′-OMe RNAs were purchased from *Eurogentec*. RNA **1**: 5′-UAAAGUG-CUUAUAGUGCAGGTAG was purchased from IBA. All residues were ribonucleotides except for the single deoxy T residue carrying an amino linker. The oligonucleotide was labeled with a Cy 5-NHS ester (*Lumiprobe*). All oligonucleotides were stored in DNA LowBind reaction tubes (*Sarstedt*). Pull-down experiments were carried out in protein LowBind reaction tubes (*Sarstedt*).

Quantification of oligonucleotides: Oligonucleotide concentrations were determined through UV spectrometry on a *nanodrop2000* (*Thermo Scientific*) using *Lambert–Beer*'s law. Extinction coefficients were calculated by a nearest neighbor model according to

literature.[55] For simplification, influences of the modifications were neglected.

Bandshift Assay

The oligonucleotides (1 μM) were mixed in a volume of 10 μL of incubation buffer (100 mM KCl, 2 mM $MgCl_2$, 50 mM *Tris*•HCl pH 8). The adaptor molecule (1 or 2 μM) was added, and the samples were incubated for 16 h at room temperature (RT). Prior to electrophoresis, loading buffer (40% sucrose, 0.25 *Crocein Orange G*) was added. The gel (16% native PAGE) was subsequently stained with *SYBR Gold* (*Thermo Fisher Scientific*).

Thermal Denaturation of Oligonucleotide Duplexes

The oligonucleotides (1 μM of each strand) were preincubated in 1 mL of incubation buffer (100 mM KCl, 2 mM $MgCl_2$, 50 mM *Tris*•HCl pH 8) overnight at 37 °C. Melting points were measured with a UV-VIS spectrometer (*Evolution 300*, *Thermo Scientific*) by using a 1 mL cuvette (*Hellma Analytics*) with a path length of 1 cm. The cell holder was controlled thermoelectrically, while the temperature of the solution was measured independently. The heating and cooling rates were of 1 °C/min. The change of UV absorption at 260 nm was measured in a range from 20 °C to 90 °C in three to five cycles. The resulting curves were fitted separately by OriginLabs using a sigmoidal fit. The final melting points were determined by averaging (for plots see *Supporting Information*).

Preparation of Cytosolic Extract[56]

HeLa S3 cells were grown in suspension in serum-free *ISF-1* Medium (*PAN-Biotech*, *P04-995968*). Culture conditions were 37 °C and 5% CO_2 with saturating humidity. The cells were harvested and the resulting suspension (550 mL) was centrifuged for 20 min at 4000 × *g* at 4 °C. The resulting pellet was two times resuspended with 50 mL PBS-buffer and centrifuged for 5 min at 1000 × *g* at 4 °C. Afterwards, the pellet (4.2 g wet weight) was resuspended in 4.2 mL of buffer A (10 mM HEPES (pH 7.5), 1.5 mM $MgCl_2$, 10 mM KCl) and centrifuged again (5 min, 1000 × *g*, 4 °C). The pellet was resuspended in the same buffer (4.2 mL) and incubated on ice for 30 min. Afterwards, the suspension was centrifuged for 30 min at 18000 × *g* at 4 °C. The supernatant was collected and then stored at −80 °C. Prior to freezing 30 μL/mL 3 M KCl und 0.5 μL/mL 1 M $MgCl_2$ were added. Cytosolic extracts had an average protein concentration of 5.2 mg/mL determined with the *Bradford* assay.

Pull-Down Experiments

Loading: Streptavidin-coated magnetic-beads (600 μL aliquot; binding capacity 0.75 pmol/μL) were washed three times with 0.5X SSPE-buffer (5 mM sodium dihydrogen phosphate; 0.5 mM EDTA and 75 mM sodium chloride). Afterwards, a solution of biotinylated oligonucleotides (2 μM) in 0.5X SSPE-buffer (450 μL) with 10% *Roti*®-Block (*Roth*) was added. The suspension was incubated overnight at RT. After the beads were collected with a magnetic stand, the supernatant was removed, and the beads were washed three times with 0.5X SSPE-buffer.

Fluorescence pull-down: An aliquot of beads loaded with capture RNA (100 nM) was suspended in 50 μL of incubation buffer (100 mM KCl, 2 mM $MgCl_2$, 50 mM *Tris*•HCl pH 8.0, 10% *Roti*®-Block). RNA **1** (100 nM) was added followed by the adaptor **2** or **4** (0–600 nM). The mixture was incubated for 1 h at RT, while the beads were kept in suspension. The beads were then washed five times with the same buffer. To separate the strands, 0.5X SSPE-buffer was added followed by the addition of 3 μL of 0.1 M NaOH. After 30 min, the suspension was transferred in a black 96 well microtiter plate (*Corning costar*) and the fluorescence was recorded (λ_{ex} = 649 nm, λ_{em} = 670 nm, *Tecan Safire II*).

Western blot, general procedure: An aliquot of magnetic beads loaded with oligonucleotides was incubated in cytosolic lysate at RT for 1 to 3 h. After incubation, the beads were washed five times with incubation buffer. Then 6 μL of 2x *Laemmli*-buffer (100 mM *Tris*•HCl pH 6.8, 20% glycerol 4% SDS, 200 mM DTT, 0.1% bromophenol blue) were added and the mixture was heated to 90 °C for 5 to 10 min. The samples were analyzed by SDS-PAGE (6% or 8% stacking, 8% or 10% resolving gel). Gels were run at 100 to 120 V. After electrophoresis, proteins were transferred to a PVDF membrane at 8 W for 30 min. The membrane was blocked with 10% *Roti*®-Block or 0.5% casein (*Hammarsten* grade) overnight at 4 °C. Afterwards, the membrane was incubated with the primary antibody (*Sino Biological*, *11079-T36*) diluted 1:200 or 1:400 in *Tris*-buffered saline with either 10% *Roti*®-Block or 0.5% casein (*Hammarsten* grade). The membrane was washed three times with *Tris*-buffered saline containing 0.1% *Tween 20* followed by addition of the dye-labeled secondary antibody (*ThermoFisher*

Scientific, *35563*) in a dilution of 1:4000 or the AP-linked antibody (*Cell Signaling*, *S7054*) in a dilution of 1:2000. In the first case, the fluorescence was detected using a *FUSION Xpress™ Multi-Imaging System* and in the second case, a colorimetric stain was performed with NBT and BICP.

Pull-down, test for selectivity (*Figure 7*): An aliquot of beads loaded with capture LNA **8** (1 μM) was incubated in 100 μL cytosolic lysate for 1 h at RT. The beads were collected using a magnetic stand, the supernatant was transferred to another aliquot of beads loaded with LNA **8** and incubation was repeated. The beads were collected again, and the supernatant was transferred to an aliquot of beads loaded with capture LNA **9**. Then, the beads were incubated for 1 h, and the procedure was repeated with another aliquot of beads loaded with LNA **9**. After that the beads were treated as described in the *General Procedure* above. In this case, the AP-linked secondary antibody was used.

Redirection of miR-20a (*Figure 8*): An aliquot of beads loaded with capture 2′-OMe-RNA **3** (100 nM) was suspended in 300 μL cytosolic lysate containing 2 mM dithiothreitol (DDT). The adaptor molecule **2** (100 nM) was added, and the mixture was incubated for 3 h at RT, while the beads were kept in suspension. Afterwards the beads were treated following the general procedure for Western blots. The dye-labeled secondary antibody (see above) was used.

Supporting Information

Supporting Information for this article is available on the WWW under https://doi.org/10.1002/cbdv.-202000272. The thermal denaturation curves related to *Figure 6* are shown.

Acknowledgements

Financial support by the Federal State of Hesse (Germany) is gratefully acknowledged (LOEWE Research Cluster SynChemBio).

Author Contribution Statement

M. B., *L. T.*, *R. K. H.* and *M. W. G.* planned the study. *M. B.* and *L. T.* conducted the experiments. *U. S.* and *E. K.* prepared the HeLa extracts. *M. B.*, *L. T.*, *R. K. H.* and *M. W. G.* wrote the manuscript.

References

[1] R. C. Lee, R. L. Feinbaum, V. Ambros, 'The C. elegans Heterochronic Gene *lin-4* Encodes Small RNAs with Antisense Complementarity to *lin-14*', *Cell* **1993**, *75*, 843–854.
[2] D. P. Bartel, 'MicroRNAs: Genomics, Biogenesis, Mechanism, and Function', *Cell* **2004**, *116*, 281–297.
[3] L. He, G. J. Hannon, 'MicroRNAs: small RNAs with a big role in gene regulation', *Nat. Rev. Genet.* **2004**, *5*, 522–531.
[4] A. S. Flynt, E. C. Lai, 'Biological principles of microRNA-mediated regulation: shared themes amid diversity', *Nat. Rev. Genet.* **2008**, *9*, 831–842.
[5] D. P. Bartel, 'MicroRNAs: Target Recognition and Regulatory Functions', *Cell* **2009**, *136*, 215–233.
[6] M. Ghildiyal, P. Zamore, 'Small silencing RNAs: an expanding universe', *Nat. Rev. Genet.* **2009**, *10*, 94–108.
[7] M. R. Fabian, N. Sonenberg, W. Filipowicz, 'Regulation of mRNA Translation and Stability by microRNAs', *Annu. Rev. Biochem.* **2010**, *79*, 351–379.
[8] R. C. Wilson, J. A. Doudna, 'Molecular Mechanisms of RNA Interference', *Annu. Rev. Biophys.* **2013**, *42*, 217–239.
[9] T. Treiber, N. Treiber, G. Meister, 'Regulation of microRNA biogenesis and its crosstalk with other cellular pathways', *Nat. Rev. Mol. Cell Biol.* **2019**, *20*, 5–20.
[10] C. J. Stavast, S. J. Erkeland, 'The Non-Canonical Aspects of MicroRNAs: Many Roads to Gene Regulation', *Cells* **2019**, *8*, 1465.
[11] A. Fire, S. Xu, M. K. Montgomery, S. A. Kostas, S. E. Driver, C. C. Mello, 'Potent and specific genetic interference by double-stranded RNA in *Caenorhabditis elegans*', *Nature* **1998**, *391*, 806–811.
[12] S. M. Hammond, E. Bernstein, D. Beach, G. J. Hannon, 'An RNA-directed nuclease mediates post-transcriptional gene silencing in *Drosophila* cells', *Nature* **2000**, *404*, 293–296.
[13] P. D. Zamore, T. Tuschl, P. A. Sharp, D. P. Bartel, 'RNAi: Double-Stranded RNA Directs the ATP-Dependent Cleavage of mRNA at 21 to 23 Nucleotide Intervals', *Cell* **2000**, *101*, 25–33.
[14] S. M. Elbashir, J. Harborth, W. Lendeckel, A. Yalcin, K. Weber, T. Tuschl, 'Duplexes of 21-nucleotide RNAs mediate RNA interference in cultured mammalian cells', *Nature* **2001**, *411*, 494–498.
[15] J. Liu, M. A. Carmell, F. V. Rivas, C. G. Marsden, J. M. Thomson, J.-J. Song, S. M. Hammond, L. Joshua-Tor, G. J. Hannon, 'Argonaute2 Is the Catalytic Engine of Mammalian RNAi', *Science* **2004**, *305*, 1437–1441.
[16] G. Meister, M. Landthaler, A. Patkaniowska, Y. Dorsett, G. Teng, T. Tuschl, 'Human Argonaute2 Mediates RNA Cleavage Targeted by miRNAs and siRNAs', *Mol. Cell* **2004**, *15*, 185–197.
[17] E. Jung, Y. Seong, B. Jeon, H. Song, Y.-S. Kwon, 'Global analysis of AGO2-bound RNAs reveals that miRNAs induce cleavage of target RNAs with limited complementarity', *Biochim. Biophys. Acta Gene Regul. Mech.* **2017**, *1860*, 1148–1158.

[18] B. P. Lewis, C. B. Burge, D. P. Bartel, 'Conserved Seed Pairing, Often Flanked by Adenosines, Indicates that Thousands of Human Genes are MicroRNA Targets', *Cell* **2005**, *120*, 15–20.
[19] M. Selbach, B. Schwanhäusser, N. Thierfelder, Z. Fang, R. Khanin, N. Rajewsky, 'Widespread changes in protein synthesis induced by microRNAs', *Nature* **2008**, *455*, 58–63.
[20] D. Baek, J. Villén, C. Shin, F. D. Camargo, S. P. Gygi, D. P. Bartel, 'The impact of microRNAs on protein output', *Nature* **2008**, *455*, 64–71.
[21] R. C. Friedman, K. K.-H. Farh, C. B. Burge, D. P. Bartel, 'Most mammalian mRNAs are conserved targets of microRNAs', *Genome Res.* **2009**, *19, 92–105*.
[22] S. M. Hammond, 'MicroRNAs as oncogenes', *Curr. Opin. Genet. Dev.* **2006**, *16*, 4–9.
[23] S. Volinia, G. A. Calin, C.-G. Liu, S. Ambs, A. Cimmino, F. Petrocca, R. Visone, M. Iorio, C. Roldo, M. Ferracin, R. L. Prueitt, N. Yanaihara, G. Lanza, A. Scarpa, A. Vecchione, M. Negrini, C. C. Harris, C. M. Croce, 'A microRNA expression signature of human solid tumors defines cancer gene targets', *Proc. Natl. Acad. Sci. USA* **2006**, *103*, 2257–2261.
[24] R. Garzon, G. Marcucci, C. M. Croce, 'Targeting microRNAs in cancer: rationale, strategies and challenges', *Nat. Rev. Drug Discovery* **2010**, *9*, 775–789.
[25] J. T. Mendell, 'miRiad Roles for the miR-17-92 Cluster in Development and Disease', *Cell* **2008**, *133*, 217–222.
[26] J. Krützfeldt, N. Rajewsky, R. Braich, K. G. Rajeev, T. Tuschl, M. Manoharan, M. Stoffel, 'Silencing of microRNAs in vivo with 'antagomirs'', *Nature* **2005**, *438*, 685–689.
[27] G. Meister, M. Landthaler, Y. Dorsett, T. Tuschl, 'Sequence-specific inhibition of microRNA and siRNA-induced RNA silencing', *RNA* **2004**, *10*, 544–550.
[28] G. Hutvágner, M. J. Simard, C. C. Mello, P. D. Zamore, 'Sequence-Specific Inhibition of Small RNA Function', *PLoS Biol.* **2004**, *2*, e98.
[29] J. Elmén, M. Lindow, S. Schütz, M. Lawrence, A. Petri, S. Obad, M. Lindholm, M. Hedtjärn, H. F. Hansen, U. Berger, S. Gullans, P. Kearney, P. Sarnow, E. M. Straarup, S. Kauppinen, 'LNA-mediated microRNA silencing in non-human Primates', *Nature* **2008**, *452*, 896–900.
[30] E. M. Small, E. N. Olson, 'Pervasive roles of microRNAs in cardiovascular biology', *Nature* **2011**, *469*, 336–342.
[31] E. van Rooij, E. N. Olson, 'MicroRNA therapeutics for cardiovascular disease: opportunities and obstacles', *Nat. Rev. Drug Discovery* **2012**, *11*, 860–872.
[32] E. van Rooij, S. Kauppinen, 'Development of microRNA therapeutics is coming of age', *EMBO Mol. Med.* **2014**, *6*, 851–864.
[33] R. Rupaimoole, F. J. Slack, 'MicroRNA therapeutics: towards a new era for the management of cancer and other diseases', *Nat. Rev. Drug Discovery* **2017**, *16*, 203–221.
[34] S. Grijalvo, A. Alagia, A. F. Jorge, R. Eritja, 'Covalent Strategies for Targeting Messenger and Non-Coding RNAs: An Updated Review on siRNA, miRNA and antimiR Conjugates', *Genes* **2018**, *9*, 74.
[35] P. Trang, J. F. Wiggins, C. L. Daige, C. Cho, M. Omotola, D. Brown, J. B. Weidhaas, A. G. Bader, F. J. Slack, 'Systemic Delivery of Tumor Suppressor microRNA Mimics Using a Neutral Lipid Emulsion Inhibits Lung Tumors in Mice', *Mol. Ther.* **2011**, *19*, 1116–1122.
[36] A. F. Ibrahim, U. Weirauch, M. Thomas, A. Grünweller, R. K. Hartmann, A. Aigner, 'MicroRNA Replacement Therapy for miR-145 and miR-33a Is Efficacious in a Model of Colon Carcinoma', *Cancer Res.* **2011**, *71*, 5214–5224.
[37] A. L. Kasinski, F. J. Slack, 'miRNA-34 Prevents Cancer Initiation and Progression in a Therapeutically Resistant K-ras and p53-Induced Mouse Model of Lung Adenocarcinoma', *Cancer Res.* **2012**, *72*, 5576–5587.
[38] N. Hosseinahli, M. Aghapour, P. H. G. Duijf, B. Baradaran, 'Treating cancer with microRNA replacement therapy: A literature review', *J. Cell. Physiol.* **2018**, *233*, 5574–5588.
[39] J. Martinez, A. Patkaniowska, H. Urlaub, R. Lührmann, T. Tuschl, 'Single-Stranded Antisense siRNAs Guide Target RNA Cleavage in RNAi', *Cell* **2002**, *110*, 563–574.
[40] T. Holen, M. Amarzguioui, E. Babaie, H. Prydz, 'Similar behaviour of single-strand and double-strand siRNAs suggests they act through a common RNAi pathway', *Nucleic Acids Res.* **2003**, *31*, 2401–2407.
[41] D. A. Braasch, S. Jensen, Y. Liu, K. Kaur, K. Arar, M. A. White, D. R. Corey, 'RNA Interference in Mammalian Cells by Chemically-Modified RNA', *Biochemistry* **2003**, *42*, 7967–2975.
[42] A. H. S. Hall, J. Wan, E. E. Shaughnessy, B. Ramsay Shaw, K. A. Alexander, 'RNA interference using boranophosphate siRNAs: structure–activity relationships', *Nucleic Acids Res.* **2004**, *32*, 5991–6000.
[43] W. F. Lima, T. P. Prakash, H. M. Murray, G. A. Kinberger, W. Li, A. E. Chappell, C. S. Li, S. F. Murray, H. Gaus, P. P. Seth, E. E. Swayze, S. T. Crooke, 'Single-Stranded siRNAs Activate RNAi in Animals', *Cell* **2012**, *150*, 883–894.
[44] D. Yu, H. Pendergraff, J. Liu, H. B. Kordasiewicz, D. W. Cleveland, E. E. Swayze, W. F. Lima, S. T. Crooke, T. P. Prakash, D. R. Corey, 'Single-Stranded RNAs Use RNAi to Potently and Allele-Selectively Inhibit Mutant Huntingtin Expression', *Cell* **2012**, *150*, 895–908.
[45] N. T. Schirle, G. A. Kinberger, H. F. Murray, W. F. Lima, T. P. Prakash, I. J. MacRae, 'Structural Analysis of Human Argonaute-2 Bound to a Modified siRNA Guide', *J. Am. Chem. Soc.* **2016**, *138*, 8694–8697.
[46] V. Kotikam, J. A. Viel, E. Rozners, 'Synthesis and Biological Activity of Short Interfering RNAs Having Several Consecutive Amide Internucleoside Linkages', *Chem. Eur. J.* **2020**, *26*, 685–690.
[47] G. Chorn, M. Klein-McDowell, L. Zhao, M. A. Saunders, W. M. Flanagan, A. T. Willingham, L. P. Lim, 'Single-stranded microRNA mimics', *RNA* **2012**, *18*, 1796–1804.
[48] M. Matsui, T. P. Prakash, D. R. Corey, 'Argonaute 2-dependent Regulation of Gene Expression by Single-stranded miRNA Mimics', *Mol. Ther.* **2016**, *24*, 946–955.
[49] X. Wang, X. Xiao, B. Zhang, J. Li, Y. Zhang, 'A self-assembled peptide nucleic acid–microRNA nanocomplex for dual modulation of cancer-related microRNAs', *Chem. Commun.* **2019**, *55*, 2106–2109.
[50] S. Jonas, E. Izaurralde, 'Towards a molecular understanding of microRNA-mediated gene silencing', *Nat. Rev. Genet.* **2015**, *16*, 421–433.
[51] M. Thomas, K. Lange-Grünweller, U. Weirauch, D. Gutsch, A. Aigner, A. Grünweller, R. K. Hartmann, 'The proto-oncogene Pim-1 is a target of miR-33a', *Oncogene* **2012**, *31*, 918–928.
[52] F. Zellmann, L. Thomas, U. Scheffer, R. K. Hartmann, M. W. Göbel, 'Site-Specific Cleavage of RNAs Derived from the

PIM1 3′-UTR by a Metal-Free Artificial Ribonuclease', *Molecules* **2019**, *24*, 807.

[53] C. F. Flores-Jasso, W. E. Salomon, P. D. Zamore, 'Rapid and specific purification of Argonaute-small RNA complexes from crude cell lysates', *RNA* **2013**, *19*, 271 – 279.

[54] V. K. Mayya, T. F. Duchaine, 'On the availability of microRNA-induced silencing complexes, saturation of microRNA-binding sites and stoichiometry', *Nucleic Acids Res.* **2015**, *43*, 7556 – 7565.

[55] D. M. Gray, S.-H. Hung, K. H. Johnson, 'Absorption and Circular-Dichroism Spectroscopy of Nucleic-Acid Duplexes and Triplexes', *Methods Enzymol.* **1995**, *246*, 19 – 34.

[56] J. D. Dignam, R. M. Lebovitz, R. G. Roeder, 'Accurate transcription initiation by RNA polymerase II in a soluble extract from isolated mammalian nuclei', *Nucleic Acids Res.* **1983**, *11*, 1475 – 1489.

Received April 7, 2020
Accepted May 19, 2020

